Iranian Journal of Medical Physics

ijmp.mums.ac.ir

Calculation of Inter- and Intra-Fraction Motion Errors at External Radiotherapy Using a Markerless Strategy Based on Image Registration Combined with Correlation Model

Payam Samadi Miandoab[1], Ahmad Esmaili Torshabi [2], Sohelia Parandeh [2]

1. Faculty of Energy Engineering and Physics, Amirkabir University of Technology, Tehran, Iran
2. Department of Electrical and Computer Engineering, Medical Radiation Group, Graduate University of Advanced Technology, Kerman, Iran

ARTICLE INFO

Article type:
Original Article

Article history:
Received: Apr 15, 2018
Accepted: Jun 18, 2018

Keywords:
Image Processing
Image Guided Radiation Therapy (IGRT)
Patient Positioning

ABSTRACT

Introduction: A new method based on image registration technique and an intelligent correlation model to calculate. The present study aimed to propose inter- and intra-fraction motion errors in order to address the limitations of conventional Patient positioning methods.

Material and Methods: The configuration of the markerless method was accomplished by using four-dimensional computed tomography (4DCT) datasets. Firstly, the MeVisLab software package was used to extract a three-dimensional (3D) surface model of the patient and determine the tumor location. Then, the patient-specific 3D surface model which also included the breathing phases was imported into the MATLAB software package in order to define several control points on the thorax region as virtual external markers. Finally, based on the correlation of breathing signals/patient position with breathing signals/tumor coordinate, an adaptive neuro fuzzy inference system was proposed to both verify and align the inter- and intra-fraction motion errors in radiotherapy, if needed. In order to validate the proposed method, the 4DCT data acquired from four real patients was considered.

Results: Final results revealed that our hybrid configuration method was capable of aligning patient setup with lower uncertainties, compared to other available methods. In addition, the 3D root-mean-square error has been reduced from 5.26 to 1.5 mm for all patients.

Conclusion: In this study, a markerless method based on the image registration technique in combination with a correlation model was proposed to address the limitations of the available methods, including dependence on operator's attention, use of passive markers, and rigid-only constraint for patient setup.

►*Please cite this article as:*
Samadi Miandoab P, Esmaili Torshabi A, Parandeh S. Calculation of Inter- and Intra-Fraction Motion Errors at External Radiotherapy Using a Markerless Strategy Based on Image Registration Combined with Correlation Model. Iran J Med Phys 2019; 16: 224-231. 10.22038/ijmp.2018.30477.1348.

Introduction

In external beam radiotherapy, a successful radiotherapy involves the use of a uniform dose distribution within the target volume with a minimum dose to the surrounding tissue volumes. However, in clinical applications, a number of limitations result in differences in the planned and delivered doses to the patient. In the recent attempts having targeted toward the achievement of a successful radiotherapy, two steps have been proposed. These steps include the localization and delineation of the tumor at the treatment planning process and a three-dimensional (3D) dose distribution in the tumor volume [1].

However, these steps involve challenging issues when used for the treatment of dynamic tumors located in the thorax region of the patient's body. These tumors move because of intra-fractional (i.e., the breathing phenomena, heartbeat, and gastrointestinal motions) and inter-fractional (i.e., patient verification) motions. In order to compensate the intra-fractional motion errors, several strategies have been implemented, such as breath-holding, real-time tumor-tracking, and respiratory motion gating [2-5].

In the external beam radiotherapy, serious concerns have been raised due to inter- and intra-fraction motion errors in both treatment stages. Since the tumor position and its geometrical structure change at each fraction of irradiation, these errors are remarkable and cannot be neglected. This issue is especially challenging for long-lasting treatments, such as the stereotactic body radiation therapy, which involves the delivery of hypofractionated doses to small treatment fields.

In order to compensate for the inter- and intra-fraction motion errors, the computer-aided systems working through modeling and simulation have become increasingly important in different radiotherapy stages ranging from the tumor

*Corresponding Author: Tel: +989366440159; Email: p.samadi1989@gmail.com

localization to dose delivery. As an example, the optoelectronics or laser spot scanning are practical techniques to minimize inter-fraction motion errors, which are capable of filling the gap between a personalized treatment plan and irradiation setup uncertainties [1].

Although these techniques prepare an acceptable trade-off between expedite and patient positioning accuracy, their efficacy are totally dependent on operator's attention due to lacking a quantitative online control over the quality of the particular repositioning. To solve this issue, it is required to increase the number of surface control points and compute continuous surface modifications during the irradiation of the body area. In order to fulfill this need, a patient verification system was proposed based on the detection and registration of the entire irradiated body surface, such as AlignRT, Radio Cameras, and C-Rad sentinel as an optical system [6-9]. These techniques allow to address the limitations of the optoelectronic passive marker and the rigid-body setup errors. However, the main drawback of these techniques is that they potentially increase the length of treatment process [10-13]. As a second drawback, these techniques only track the patient's surface, and an additional system is necessary to calculate the correction between the alignment of the patient and the initial position [10-13]. As a final drawback, the body surface detection system is unable to gather signals from fluctuating reflective surfaces, such as hair and clothing [10-13].

In this study, a markerless method based on the image registration technique and an intelligent correlation model was proposed to verify both inter- and intra-fraction motion errors. This study included three main sections. In the first step, four-dimensional computed tomography (4DCT) data were imported into the MeVislab software to extract a 3D surface model of the patient and determine the location of the tumor volume during respiration phases as initial patient positioning (i.e., benchmark position).

In the second stage, the 3D surface model of the patient extracted from all phases was imported into the MATLAB software to define several control points on the thorax surface as external marker position. In addition, the information of nine control points and tumor position was synchronized as a function of the patient breathing at different cycles. Finally, a correlation model was used in real-time patient positioning with tumor tracking.

The configuration of the proposed model was accomplished in the both treatment stages. The nine control points (i.e., external markers) were used as the input data of the correlation model to verify the rigid and non-rigid body setup errors. In this study, the correlation model was developed under the performance of an adaptive neuro-fuzzy inference system (ANFIS).

After the initial setup, the results of the ANFIS model facilitated the comparison of the treatment position with benchmark position to finally apply the correction parameters to the treatment couch as necessary. The proposed strategy was validated by using reference 4DCT datasets obtained from four real patients. The obtained results indicated that the markerless model used in this study was able to not only detect and reduce setup errors, but also provide a high reliability data for patient positioning. In addition, the intelligent model (ANFIS) used in this study rendered sensitive method to verify the inter- and intra-fraction motion errors.

Materials and Methods

Image Acquisition

A subset of the data previously collected by David Sarrut regarding image acquisition and post-processing procedures were used in this study [14-16]. In order to acquire images, the 10 Slice Brilliance CT Big Bore Oncology™ configuration (Philips Medical Systems, Cleveland, OH) was considered. The data about patient breathing was acquired by using the associated Pneumo Chest bellows™ (Lafayette Instrument, Lafayette, IN). In addition, the parameters used to determine this asset included a tube tension of 120 kV, field view of 500 mm, exposure of 400 mA/slice, gantry rotation time of 0.5 sec, collimation of 16×1.5 mm, and pitch of 0.15. Table 1 presents the information of four patients, including tumor location, diaphragm movements in the superior-inferior (SI) direction, and dimension of the 4DCT acquisition by protocols.

Image Registration Technique

Image registration technique is a useful and validated method for various practical applications, such as image processing and analysis, anatomical atlas building, pattern recognition, anatomy segmentation, computer vision, and knowledge discovery.

Table 1. Patient information on tumor location, diaphragm movement in the superior-inferior direction, and dimension of the four-dimensional computed tomography acquisition protocols

Patient	Image dimension	Pixel dimension [mm]	Tumor type	Diaphragm motion amplitude (cm)
Patient #1	512*512*169	0.97*0.97*2	LUL	1.25
Patient #2	512*512*170	0.87*0.87*2	LLL	1.00
Patient #3	512*512*187	0.78*0.78*2	RML	1.25
Patient #4	512*512*161	1.17*1.17*2	RUL	0.75

LLL: left lower lobe, LUL: left upper lobe, RML: right middle lobe, RUL: right upper lobe

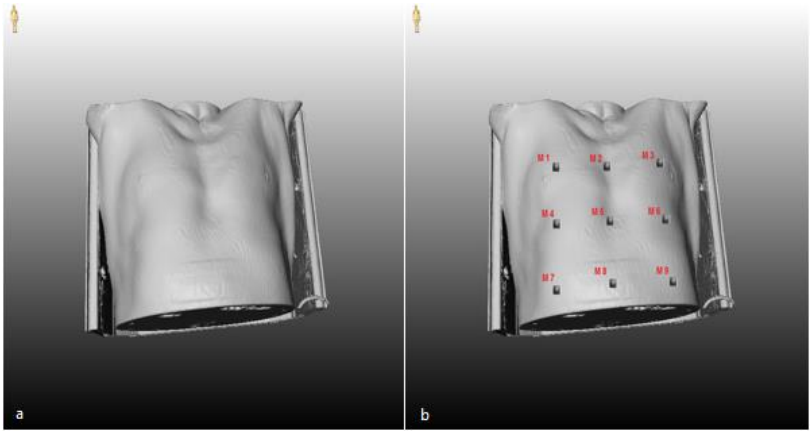

Figure 1. a) Three-dimensional surface reconstruction by using MeVisLab software based on region growing techniques and morphological operators, b) distribution of nine control points on patient surface as virtual external markers by MATLAB software

In this study, the MeVisLab package was used as a surface detection model to reduce the cost of treatment and compensate the lack of accessibility to AlignRT or Radio Cameras instrument. The use of MeVisLab package (available on www.mevislab.de, MeVis Research GmbH, Bremen, Germany) in image registration techniques has been validated [17, 18].

In the pretreatment stage, the 3D surface reconstruction was performed using the MeVisLab package, which uses region growing technique and the morphological operator. Both segmentation techniques were applied to extract the 3D surface model of the patient and tumor location from the 4DCT dataset [19].

The triangulated 3D surface models were generated based on the segmented data (Figure 1-a). Then, the 3D surface model of the patient was imported to the MATLAB software (Math Works Inc., Natick, MA) to define several control points on the thorax surface as external marker positions. The determination of the location of each nine control points on the surface of the chest and abdominal regions was accomplished based on the literature [2, 3, 20, 21]. Following the previous studies, in order to evaluate the optimum location of external markers, nine sub-regions were determined on the thorax region. The nine control points were chosen from nine sub-regions on the thorax, each of which represented virtual external markers.

In addition, the selected external markers indicated high motion amplitudes and high motion correlations during respiration with the corresponding reference. By synchronizing these data, the nine control points on the surface of the chest and abdominal regions were correlated with the pulmonary tumor position as a function of the patient breathing cycles [8, 22, 23]. It should be noted that each of the 3D surfaces (i.e., breathing cycle phases) created from the 4DCT dataset was unique for each patient.

The scheme of the depicted points started from the abdominal region with an averagely 5-cm distance in the vertical and horizontal directions (Figure 1-b). The given points in this figure proposed in the spatial scheme were divided into nine regions, namely right upper lobe (M1), middle upper lobe (M2), left upper lobe (M3), right middle lobe (M4), XIPHOID (M5), Left middle lobe (M6), right down lobe (M7), navel upper (M8), and left down lobe (M9).

Adaptive neuro-fuzzy inference system-based correlation model

There are some issues that should be kept in mind when using an intelligent model. In this regard, the importance degree is utilized in the intelligent model which must be clarified. It is evident that the position information of the surface markers is strongly correlated with patient position or tumor location. Clinically, it is necessary and desirable to use a consistent model for the real-time re-alignments of patient position in a satisfactory degree [8, 22, 23]. The robustness of ANFIS model allows for overcoming the limitations of the conventional methods [10-13].

As mentioned previously, the image registration technique is used to address the limitations of the opto-electronic passive marker and rigid-body setup errors. However, their real-time application which includes online detection and non-rigid deformations seem to be impractical [6-9]. In order to address the limitations of the previous methods, ANFIS model has been proposed to correlate the new external breathing signals and the tumor position.

Accordingly, we developed ANFIS as a correlation learning-based model by using the fuzzy logic toolbox of the MATLAB software [18]. To this end, the abilities of the fuzzy system in combination with the numeric power of the neural network system were assembled in the ANFIS model as a powerful tool in the modeling of numerous processes. Furthermore, in order to extract fuzzy rules with a high variable range, an adaptive rule-based AFNIS model was constructed to select and extract the fuzzy rules from the input/output dataset, where the same calculations are difficult or impossible to be performed with the normal mathematic approaches [18, 24].

In this study, the robustness of the ANFIS model was used in both online detection and non-rigid setup.

The architecture of the ANFIS model consists of five layers, nine rules, and nine Gaussian membership functions by implementing if-then rules (numbers of rules are equal to the numbers of clusters) using AND/OR operator in the antecedent and consequent parts of the fuzzy inference system. In addition, de-fuzzification, as the final step, was achieved by centroid calculation method.

The fuzzy inference method, which is based on Sugeno-type and fuzzy c-means, was considered in the initial data clustering. In the fuzzy c-means method, each data point with a specific membership grade can potentially belong to every cluster in the dataset which is determined by its distance from the cluster centers. In this regard, each data point in the dataset that is closer to the cluster centers has a high membership grade in opposition to the data points that are far from the cluster centers that have a lower grade [9, 18, 24-26].

The present study was targeted toward answering to the two aforementioned issues by utilizing a hybrid configuration method. The main objective of this study was to present a markerless study based on image registration technique in combination with an intelligent model in order to facilitate online detection for both rigid and non-rigid patient body setup. Figure 2 illustrates the workflow of the proposed method. To this end, firstly, the image registration technique (MeVisLab software) was used to extract the tumor location and entire irradiated body surface from the 4DCT over the patient breathing. The initial patient setup as benchmark position included the 3D surface of the thorax region and tumor location.

Secondly, the 3D surface model was given to the MATLAB software to define several control points on the extracted thorax surface as virtual external markers. In addition, the information on breathing signals/patient position and breathing signals/tumor location were synchronized and correlated as a function of the patient breathing cycles. Finally, an intelligent model was proposed based on adaptive neuro-fuzzy inference system to use the correlated data in patient verification with real-time tumor tracking or gated radiotherapy. Moreover, in the pre-treatment step, the results of our model allowed us to determine the treatment position and compare it with the benchmark position. This facilitated the induction of corrections to the treatment couch, if necessary.

To test and evaluate the markerless method, the root mean square error (RMSE) was expressed between the performance of intelligent ANFIS model and benchmarked dataset according to the following formula (1):

$$RMSE = \sqrt{\frac{1}{N}\sum_{i=1}^{N}(A_i - P_i)^2} \quad (1)$$

Where N is the number of the predicted samples, A_i is the i_{th} actual output in the dataset, and P_i is the i_{th} predicted output by the model.

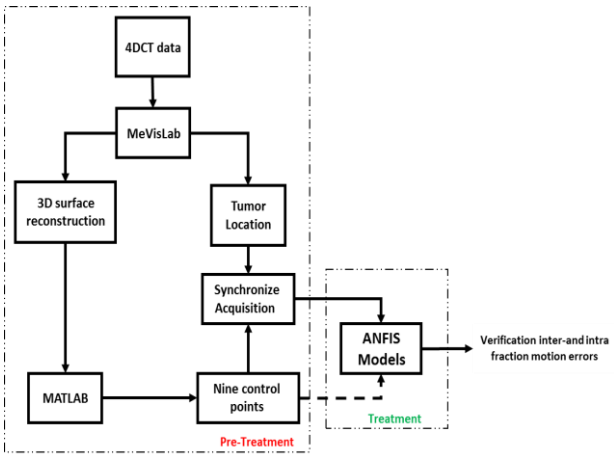

Figure 2. Work flow of the implementation of markerless method based on image registering technique and intelligent models (ANFIS) to verify inter- and intra-fraction motion errors

Results

The algorithm was tested and validated by using nine control points acquired by the 3D surface model of the patient from the 4DCT scanner dataset. In order to construct a high-accuracy patient positioning system, there are a couple of items, such as systemic availability and practical applications, which must be taken into account. In the current study, the new signal breathing was correlated with the tumor location developed under the performance of our ANFIS model to verify patient positioning and enable tumor tracking.

During the treatment procedure, the information of nine control points was used as the input data of ANFIS model, and patient alignment was applied to the treatment couch, if necessary. Figure 3 displays the RMSEs calculated between the desired output (initial patient position) at ten fractions of radiotherapy treatment course and model outputs (patient verification by the ANFIS model) while no patient alignment occurred by the operator.

The proposed machine learning algorithm, the ANFIS model, requires to use nine control points as the virtual external markers to align the patient position. This strategy was considered to improve the treatment quality by avoiding operator from depending on the selected skin markers. Furthermore, the use of nine control points on the thorax surface provided better correlation with tumor position than the utilization of one simple point of external marker.

Based on our previous study about the extended cardiac and torso of the XCAT phantom and real patients [3, 20, 21, 27, 28], due to negligible displacement motion data in the left-right (LR) direction, the LR direction was eliminated from the total database. Furthermore, the motion dataset included anterior-posterior (AP) and superior-inferior (SI) directions. In this study, the effect of the roto-translation parameters was considered to implement patient alignment correctly (Table 2).

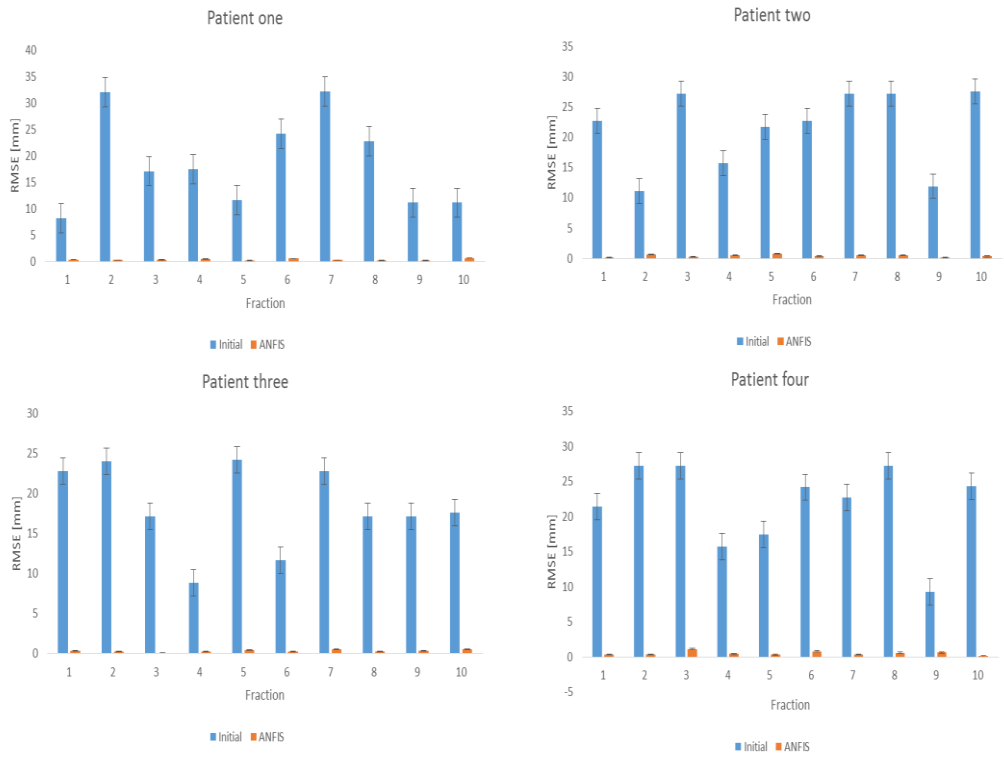

Figure 3. Representation of three-dimensional root mean square errors by the ANFIS model as patient verification against the initial patient position (i.e., benchmark position)

Table 2. Effect of roto-translation parameters on accuracy in the performance of ANFIS model

Patient	RMSE (mm) rotation	RMSE (mm) torsion	RMSE (mm) SI direction	RMSE (mm) LR direction	RMSE (mm) AP direction
	ANFIS	ANFIS	ANFIS	ANFIS	ANFIS
Patient #1	0.641	1.101	0.687	0.101	2.014
Patient #2	0.485	1.121	0.712	0.089	2.112
Patient #3	0.512	1.281	0.741	0.065	3.124
Patient #4	0.712	1.431	0.850	0.055	2.312

RMSE: root mean square error, SI: superior-inferior, AP: anterior-posterior, LR: left-right

Since the RMSEs represent the uncertainty errors of our four real cases, the ranges of accuracy in RMSE performance were varied for each patient uniquely in a case by case basis. In addition, for each case, the average RMSEs over a course of radiation treatment were 0.91, 0.97, 1.15, and 1.17 mm for patients number one, two, three, and four, respectively.

Discussion

One of the main advantages of the image-guided radiotherapy versus conventional conformal radiotherapy is the implementation of smaller radiation fields onto the tumor volume due to having more precise data regarding target localization, especially when the tumor motion is caused by respiration [29, 30]. The enhancement of accuracy in patient setup potentially facilitates margin reduction [7, 29]. Therefore, it is essential to use the feasible methods that can result in high patient setup accuracy to reduce the inter- and intra-fraction motion errors in stereotactic radiotherapy. This outcome may lead to a better protection of the healthy tissues surrounding the tumor volumes through delivering the prescribed dose to more under-controlling tumor cells.

While each circumstance for each patient setup is unique, the proposed strategies depend on patient areas, such as neck, head, breast, prostate, and abdomen. For example, Calypso is a 4D localization system, which as indicated in clinical studies is focused primarily on prostate cancer [11-13, 22]. On the other hand, the AlignRT system is related to the setup of breast cancer in patients [10, 11, 22, 31-34].

Among the available technologies for the conventional verification of the irradiation setup, several strategies may be implemented to verify the geometrical setup. These strategies include skin or laser landmarks, opto-electronic systems or laser spot scanning (body detection systems), image registration technique, hybrid configuration of control point, body frame/fiducial-based system, immobilization devices, and 7) and electronic portal imaging device. Table 3 illustrates the characteristics of these strategies [8, 10-13, 22, 23, 29-34].

Table 3. Characteristics of available technologies for patient setup verification in external beam radiotherapy

Method	Advantage	Disadvantage
Skin landmarks or laser landmarks [a,f,g,h,i, j]	Acceptable trade-off between swiftness and patient positioning	Committed operator attentions, lack of online control point, prescribed safety margins of surrounding healthy tissues
Opto-electronic systems or laser spot scanning (body detection systems) [c,d,e,f,h,i,l]	Real-time verification, immediate detection of movement subject and rigid body setup	High number of surface control point, using passive markers, non-rigid body verification
Image registration technique [b,c,f,j,k,l]	Overcoming the limits of opto-electronic passive markers	Real-time application, online detection of the breathing phase, unfeasible applications
Hybrid configuration of control point [d,h,i]	Using surface registration in combination with passive markers or laser spots	Passive markers, non-rigid body verification
Body frame/ fiducial based system [a,e,f]	Using CBCT or fluoroscopy technique to rigid and non-rigid body setup	Increasing additional received dose to the patients, lack of extension to each users situation in video-based patient localization
Immobilization devices [h,i,l]	Easy to use, easier reproducibility, improving local control, and reducing radiation side-effects, respectively	Dependence on operator's attentions, increasing the safety margins of surrounding healthy tissues
Electronic portal imaging device [c,d,e,f,m]	Implanted fiducial hardware	High cost, physical artifacts, data processing, poor image quality

[a] Reference 8, [b] Reference 10, [c] Reference 11, [d] Reference 12, [e] Reference 13, [f] Reference 22, [g] Reference 23, [h] Reference 29, [i] Reference 30, [j] Reference 31, [k] Reference 32, [l] Reference 33, [m] Reference 34

CBCT: cone beam computed tomography

In this study, in order to addresses the limitations of the available methods, a hybrid configuration method was proposed based on image registration technique and an intelligent model. The performance of our hybrid strategy included three main parts as shown in three individual figures. Figure 1-a displays the use of region growing techniques and morphological operators in order to extract the 3D surface model of patient and tumor location from the 4DCT dataset.

By importing the 3D surface model of patient into to the MATLAB software, nine control points were extracted as external markers (Figure 1-b). The synchronization of breathing signals/patient position and breathing signals/tumor location in a correlation model (Figure 2) enabled the ANFIS model to estimate patient displacement as the function of measured motion. The data acquired on patient position by ANFIS model could be compared with the benchmark position, and the obtained correction could be applied to the treatment couch.

Final results represented the performance accuracy of the markerless strategy in order to verify patient position against the initial position (i.e., benchmark position; Figure 3). The obtained RMSEs were different for each patient uniquely on a case by case basis because each patient had his/her unique breathing phases as shown in 4DCT dataset. In addition, patient setup depended on the rotation parameters (i.e., roll, pitch, and tilt) and translation parameters (i.e., shift on SI, AP, and LR directions). Each of these parameters had a unique effect on inter- and intra-fraction motion errors.

In the current study, the roles of roto-translation parameter were also taken into account (Table 2). Based on the measured roto-translation parameters (Table 2), the maximum and minimum motion displacements were occurred in the AP direction and the LR direction, respectively. Other derived results indicated that the ANFIS model could align patient position with fewer errors. Furthermore, the results showed that the average errors were reduced from 5.26 mm to 1.5 mm over all patients. Moreover, the new external breathing signals under the performance of ANFIS model could be used to reduce the sensitivity of the inter- and intra-fraction motion errors.

The main advantage of this study is the use of MeVisLab software that reduced the cost of treatment and compensated the inaccessibility to AlignRT or Radio Camera instrument. One of the drawbacks of the previous methods is that these instruments potentially increase the length of treatment process [10-13]. However, in the proposed markerless method (ANFIS model), the length of the treatment time is not potentially involved due to its online control mode. Furthermore, the markerless technique, developed based on image registration technique and an intelligent correlation model, removed the limitations related to passive markers and dependence on operator's attentions in opto-electronics techniques, laser spot scanning techniques, and immobilization techniques [6-9].

In order to overcome the second drawback of the previous methods [6-9], the information regarding breathing signals/patient position and breathing signals/tumor location was synchronized in a correlation model to track the surface of patient and reduce the necessity of additional hardware monitoring systems. In addition, the proposed correlation model (i.e., ANFIS model) was used for the online detection of both rigid and non-rigid patient body setups, while most of the previous methods are constrained to only rigid body setup [6-11].

In the present study, markerless method was used to cover both inter- and intra-fraction motion errors for the

non-rigid setup that were regarded as a challenging issue in previous studies [12, 29, 30]. In order to fulfill this challenging issue, the information of breathing signals/patient position and breathing signals/tumor location were synchronized in a correlation model (i.e., ANFIS model) to calculate the inter- and intra-fraction motion errors.

The final strength of this study is the simplicity of the proposed idea, which used the image registration technique (MeVisLab software) in combination with the intelligent correlation model (i.e., ANFIS model). However, the previous studies used additional hardware monitoring systems [10-13]. Moreover, the simplicity of the proposed idea not only reduced the cost and complexity of the motion monitoring systems, but also affected the execution time of our proposed ANFIS modeler, which is negligible regarding the data sampling rate of the motion monitoring systems or online computational time for motion management strategies at external radiotherapy [8, 10-13, 22].

Conclusion

The present study proposed a markerless technique to calculate the inter- and intra-fraction motion errors in external beam radiotherapy. This technique was validated through a simulation process by using 4DCT dataset acquired from four real patients. The proposed markerless method was assembled by image registration technique and ANFIS model in order to reduce the limitations of the available methods, such as their dependence on operator, use of real passive markers, and rigid-only constraint for patient setup. As a final suggestion, it would be better to use cone-beam computed tomography images as an input file instead of using 4DCT images in order to reduce the delivery of additional dose to patients, which is one of our next studies.

Acknowledgment

The authors would like to express their gratitude to Dr.William Paul Segars and Dr. David Surratt for the provision of the XCAT phantom and 4DCT data of four real patients, respectively.

References

1. Weiss E, Vorwerk H, Richter S, Hess CF. Interfractional and intrafractional accuracy during radiotherapy of gynecologic carcinomas: a comprehensive evaluation using the ExacTrac system. International Journal of Radiation Oncology* Biology* Physics. 2003;56(1):69-79.
2. Miyandoab PS, Torshabi AE, Nankali S. The Robustness of Various Intelligent Models in Patient Positioning at External Beam Radiotherapy.
3. Nankali S, Torshabi AE, Miandoab PS. A feasibility study on ribs as anatomical landmarks for motion tracking of lung and liver tumors at external beam radiotherapy. Technology in cancer research & treatment. 2015:1533034615595737.
4. Torshabi A, Pella A, Riboldi M, Baroni G. Targeting accuracy in real-time tumor tracking via external surrogates: a comparative study. Technology in cancer research & treatment. 2010;9(6):551-61.
5. Torshabi AE, Riboldi M, Fooladi AAI, Mosalla SMM, Baroni G. An adaptive fuzzy prediction model for real time tumor tracking in radiotherapy via external surrogates. Journal of Applied Clinical Medical Physics. 2013;14(1).
6. Chavaudra J, Bridier A. [Definition of volumes in external radiotherapy: ICRU reports 50 and 62]. Cancer radiotherapie: journal de la Societe francaise de radiotherapie oncologique. 2001;5(5):472-8.
7. Chen GT, Sharp GC, Mori S. A review of image-guided radiotherapy. Radiological physics and technology. 2009;2(1):1-12.
8. Gierga DP, Brewer J, Sharp GC, Betke M, Willett CG, Chen GT. The correlation between internal and external markers for abdominal tumors: implications for respiratory gating. International Journal of Radiation Oncology* Biology* Physics. 2005;61(5):1551-8.
9. Robert B. Fuzzy and Neural Control DISC Course Lecture notes. Delft University of Technology. 2004.
10. Cerviño LI, Pawlicki T, Lawson JD, Jiang SB. Frame-less and mask-less cranial stereotactic radiosurgery: a feasibility study. Physics in medicine and biology. 2010;55(7):1863.
11. D'Ambrosio DJ, Bayouth J, Chetty IJ, Buyyounouski MK, Price RA, Correa CR, et al. Continuous localization technologies for radiotherapy delivery: report of the American Society for Radiation Oncology Emerging Technology Committee. Practical radiation oncology. 2012;2(2):145-50.
12. Deantonio L, Masini L, Loi G, Gambaro G, Bolchini C, Krengli M. Detection of setup uncertainties with 3D surface registration system for conformal radiotherapy of breast cancer. Reports of Practical Oncology & Radiotherapy. 2011;16(3):77-81.
13. Willoughby T, Lehmann J, Bencomo JA, Jani SK, Santanam L, Sethi A, et al. Quality assurance for nonradiographic radiotherapy localization and positioning systems: Report of Task Group 147. Medical physics. 2012;39(4):1728-47.
14. Murphy K, van Ginneken B, Klein S, Staring M, de Hoop BJ, Viergever MA, et al. Semi-automatic construction of reference standards for evaluation of image registration. Medical Image Analysis. 2011;15(1):71-84.
15. Vandemeulebroucke J, Bernard O, Rit S, Kybic J, Clarysse P, Sarrut D. Automated segmentation of a motion mask to preserve sliding motion in deformable registration of thoracic CT. Medical physics. 2012;39(2):1006-15.
16. Vandemeulebroucke J, Rit S, Kybic J, Clarysse P, Sarrut D. Spatiotemporal motion estimation for respiratory-correlated imaging of the lungs. Medical physics. 2011;38(1):166-78.
17. Cordes J, Dornheim J, Preim B, Hertel I, Strauss G, editors. Pre-operative segmentation of neck CT datasets for the planning of neck dissections. Medical Imaging; 2006: International Society for Optics and Photonics.
18. Jang J-S. ANFIS: adaptive-network-based fuzzy inference system. IEEE transactions on systems, man, and cybernetics. 1993;23(3):665-85.

19. Egger J, Tokuda J, Chauvin L, Freisleben B, Nimsky C, Kapur T, et al. Integration of the OpenIGTLink Network Protocol for image-guided therapy with the medical platform MeVisLab. The International Journal of Medical Robotics and Computer Assisted Surgery. 2012;8(3):282-90.
20. Miandoab PS, Torshabi AE, Nankali S. Investigation of the optimum location of external markers for patient setup accuracy enhancement at external beam radiotherapy. Journal of Applied Clinical Medical Physics. 2016;17(6).
21. Nankali S, Torshabi AE, Miandoab PS, Baghizadeh A. Optimum location of external markers using feature selection algorithms for real-time tumor tracking in external-beam radiotherapy: a virtual phantom study. Journal of Applied Clinical Medical Physics. 2016;17(1).
22. Fayad H, Pan T, Clement JF, Visvikis D. Technical note: Correlation of respiratory motion between external patient surface and internal anatomical landmarks. Medical physics. 2011;38(6):3157-64.
23. Soete G, Van de Steene J, Verellen D, Vinh-Hung V, Van den Berge D, Michielsen D, et al. Initial clinical experience with infrared-reflecting skin markers in the positioning of patients treated by conformal radiotherapy for prostate cancer. International Journal of Radiation Oncology* Biology* Physics. 2002;52(3):694-8.
24. Verellen D, De Ridder M, Linthout N, Tournel K, Soete G, Storme G. Innovations in image-guided radiotherapy. Nature Reviews Cancer. 2007;7(12):949-60.
25. Abraham A, editor Neuro fuzzy systems: State-of-the-art modeling techniques. International Work-Conference on Artificial Neural Networks; 2001: Springer.
26. Brown M, Harris CJ. Neurofuzzy adaptive modelling and control. 1994.
27. Segars W, Mori S, Chen G, Tsui B, editors. Modeling respiratory motion variations in the 4D NCAT phantom. 2007 IEEE Nuclear Science Symposium Conference Record; 2007: IEEE.
28. Segars WP, Lalush DS, Tsui BM. Modeling respiratory mechanics in the MCAT and spline-based MCAT phantoms. IEEE Transactions on Nuclear Science. 2001;48(1):89-97.
29. Baroni G, Ferrigno G, Orecchia R, Pedotti A. Real-time opto-electronic verification of patient position in breast cancer radiotherapy. Computer Aided Surgery. 2000;5(4):296-306.
30. Frosio I, Spadea M, De Momi E, Riboldi M, Baroni G, Ferrigno G, et al. A neural network based method for optical patient set-up registration in breast radiotherapy. Annals of biomedical engineering. 2006;34(4):677.
31. Riboldi M, Baroni G, Orecchia R, Pedotti A. Enhanced surface registration techniques for patient positioning control in breast cancer radiotherapy. Technology in cancer research & treatment. 2004;3(1):51-8.
32. Riboldi M, Gierga DP, Chen GT, Baroni G. Accuracy in breast shape alignment with 3D surface fitting algorithms. Medical physics. 2009;36(4):1193-8.
33. Baroni G, Troia A, Riboldi M, Orecchia R, Ferrigno G, Pedotti A. Evaluation of methods for opto-electronic body surface sensing applied to patient position control in breast radiation therapy. Medical and Biological Engineering and Computing. 2003;41(6):679-88.
34. Boyer AL, Antonuk L, Fenster A, Van Herk M, Meertens H, Munro P, et al. A review of electronic portal imaging devices (EPIDs). Medical physics. 1992;19(1):1-16.